

Metal-rich Au-silicide nanoparticles for use in nanotechnology

E. Moyen, M. Macé, G. Agnus, A. Fleurence, T. Maroutian et al.

Citation: *Appl. Phys. Lett.* **94**, 233101 (2009); doi: 10.1063/1.3148782

View online: <http://dx.doi.org/10.1063/1.3148782>

View Table of Contents: <http://apl.aip.org/resource/1/APPLAB/v94/i23>

Published by the [American Institute of Physics](#).

Related Articles

New oxyfluoride glass with high fluorine content and laser patterning of nonlinear optical BaAlBO₃F₂ single crystal line

J. Appl. Phys. **112**, 093506 (2012)

Doping level dependent space charge limited conduction in polyaniline nanoparticles

J. Appl. Phys. **112**, 093704 (2012)

Controllable aggregates of silver nanoparticle induced by methanol for surface-enhanced Raman scattering

Appl. Phys. Lett. **101**, 173109 (2012)

CdSe quantum dots-poly(3-hexylthiophene) nanocomposite sensors for selective chloroform vapor detection at room temperature

Appl. Phys. Lett. **101**, 173108 (2012)

An "edge to edge" jigsaw-puzzle two-dimensional vapor-phase transport growth of high-quality large-area wurtzite-type ZnO (0001) nanohexagons

Appl. Phys. Lett. **101**, 173105 (2012)

Additional information on *Appl. Phys. Lett.*

Journal Homepage: <http://apl.aip.org/>

Journal Information: http://apl.aip.org/about/about_the_journal

Top downloads: http://apl.aip.org/features/most_downloaded

Information for Authors: <http://apl.aip.org/authors>

ADVERTISEMENT



Goodfellow
metals • ceramics • polymers • composites
70,000 products
450 different materials
small quantities fast

www.goodfellowusa.com

Metal-rich Au-silicide nanoparticles for use in nanotechnology

E. Moyer,^{1,a)} M. Macé,¹ G. Agnus,² A. Fleurence,² T. Maroutian,² F. Houzé,³
A. Stupakiewicz,⁴ L. Masson,¹ B. Bartenlian,² W. Wulfhekel,⁵ P. Beauvillain,² and
M. Hanbücken¹

¹CNRS, Aix-Marseille Université, CINaM-UPR3118, Campus de Luminy, 13288 Marseille Cedex 09, France

²Institut d'Electronique Fondamentale-CNRS, Université Paris-Sud, bât 220,

F-91405 Orsay Cedex, France

³Laboratoire de Génie Electrique de Paris, 11 rue Joliot Curie, Plateau de Moulon,

F-91192 Gif sur Yvette, France

⁴Laboratory of Magnetism, University of Bialystok, Lipowa 41, 15-424 Bialystok, Poland

⁵Physikalisches Institut, Universität Karlsruhe (TH), Wolfgang-Gaede-Strasse 1,
D-76131 Karlsruhe, Germany

(Received 26 January 2009; accepted 16 April 2009; published online 8 June 2009)

We present a route to functionalize chemically and magnetically silicon surfaces by a local passivation, taking advantage of Stranski–Krastanov growth mode of the Au–Si(111) system. Metal-rich Au-silicide nanoparticles, supported on a Si-rich two-dimensional Au-silicide layer, are obtained. Subsequently deposited Co is used to form magnetic nanostructures. The two Au silicides display a different chemical reactivity with Co enabling the fabrication of localized magnetic Co nanodots. These magnetic nanostructures can be aligned along step bunches of a vicinal Si(111) surface. By varying the growth parameters, the particle density can be tuned from 10^9 to the low 10^{12} dots/in.². © 2009 American Institute of Physics. [DOI: 10.1063/1.3148782]

Many applications in nanotechnology call for perfectly ordered arrays of close-to-identical nanoparticles that show specific electronic, magnetic, or chemical properties. These nanoparticles are used in various fields such as biology, material science, electronics, or information storage. For all these applications, the properties of the nanoparticles differ in a well defined and adjustable way from the properties of the supporting substrate. In magnetic data storage, the fabrication of high density monodisperse magnetic nanodots on nonmagnetic surfaces is one of the key problems already addressed by several experimental approaches. Lithographically patterned media exhibit the desired magnetic properties but those are dominated by edge effect when further decreasing in size.¹ Assembling magnetic nanostructures by self-organization methods could be the way to avoid this disadvantage. Self-assembled colloid particles allows excellent monodispersivity but poor crystallinity, resulting in insufficient magnetic properties.² Self-assembled crystalline Co nanostructures, grown on reconstructed Au(788) surfaces exhibit high densities (26 TB/in.²) but possess a blocking temperature of only 50 K.³ However, silicon is an inexpensive support preferentially used in microelectronics but poses the difficulty of systematic formation of nonmagnetic silicides at the metal-silicon interfaces. Here, we demonstrate that the mentioned demand in data storage and other domains to laterally modify more than one physical parameter can be met by a chemical functionalization. The chemically functionalized surface can then be used as a template to replicate the lateral structures to other parameters such as magnetic properties or electronic structure. Based on our knowledge of crystal growth,⁴ the idea is to prepare nanoparticles with well defined sizes, shapes, ordering, and crystal structure. The Stranski–Krastanov (SK) growth mode leads to the forma-

tion of three-dimensional (3D) islands separated by a two-dimensional (2D) layer. A difference in the chemical reactivity of the 2D thin film compared to the 3D islands is used in the present study to laterally pattern a variety of physical properties. As a model system, we chose Au epitaxy on Si(111). Gold grows on a Si(111) substrate via the SK growth mode forming two distinct Au silicides, a gold-rich silicide in the islands and a Si-rich silicide on the 2D reconstructed layer. By using vicinal surfaces as a growth template, islands can naturally be aligned on a one-dimensional (1D) lattice.

All experiments were performed in an ultrahigh vacuum (UHV) system (10^{-8} Pa range pressure) equipped with a scanning tunneling microscope (STM), several evaporation sources, low energy electron diffraction, and Auger electron spectroscopy. The vicinal Si(111) samples (*n*-type, resistivity 0.5–1 Ω cm) have a miscut of 1.5° toward the $[11\bar{2}]$ direction. Samples with dimensions of 2×12 mm² were outgassed in UHV for 12 h at 800 °C by resistive heating in the step-up direction, followed by flashing up to 1150 °C. This cleaning procedure enables the formation of equally spaced terraces, exhibiting the (7²) reconstruction, typical for clean Si(111). High purity 5N gold was evaporated from a crucible. The coverage was calibrated by imaging known Au reconstructions in the 0.1–1 ML range (1 ML is defined as 7.84×10^{14} atoms/cm²). For all experiments, the deposition rate was kept constant at 1×10^{-3} ML/s. STM images were obtained in the constant current mode. *Ex situ* transmission electron microscopy (TEM) observations were performed in a JEOL 3010 microscope at an acceleration voltage of 300 kV (point to point resolution of 0.21 nm). Samples were observed in a cross-section view along the $[1\bar{1}0]$ direction.

The atomic force microscopy (AFM) image in Fig. 1(a) shows the *ex situ* topographs of Si substrate after Au deposition (3 ML, 340 °C) in UHV. Besides the native silicon oxide film formed upon exposure to ambient air, the metallic character of the 3D Au-rich islands is clearly preserved,

^{a)}Author to whom correspondence should be addressed. Electronic mail: moyer@cinam.univ-mrs.fr.

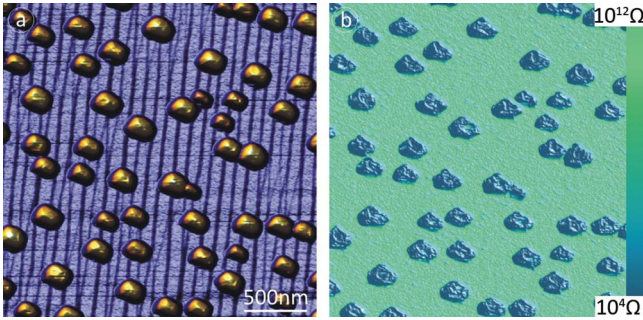


FIG. 1. (Color online) AFM image after deposition of 3 ML of Au on Si(111) at 340 °C—topographical view in (a) and local resistance in (b).

while the 2D Si-rich layer is oxidized. A different chemical reactivity toward oxidation leads to a nanopatterned electrical conductivity. As depicted in Fig. 1(b), the resistance of the film and the islands as measured with the conducting tip of an AFM shows strong variations. Six orders of magnitude higher conductivity was observed on the 3D islands compared to the surrounding silicon oxide film. This behavior results from a different chemical composition. While the thin SiAu wetting layer is oxidized leading to large local resistances of an oxide, the 3D gold-silicide islands stay metallic, which indicates a low reactivity due to a high Au content.⁵

A detailed study on the atomic level of the crystalline structure of these Au–Si islands was performed by a combined STM and TEM analysis. Islands with faceted and hemispherical shapes were prepared in UHV by varying the Au coverage and deposition temperature. The topographic STM image in Fig. 2(a) shows a typical faceted island after Au deposition (1.5 ML, 400 °C). It is truncated by a hexagonal facet on top and consists of six facets that are inclined by about 35° from the [111] direction toward the [112̄] direction of the substrate. A mesh of atoms with a centered unit cell of $0.79 \times 0.83 \text{ nm}^2$ [white arrows in Fig. 2(a) and schematic view in Fig. 2(c)] was observed on the tilted facets. From the 35° tilt of the facets, an interplane distance of 0.47

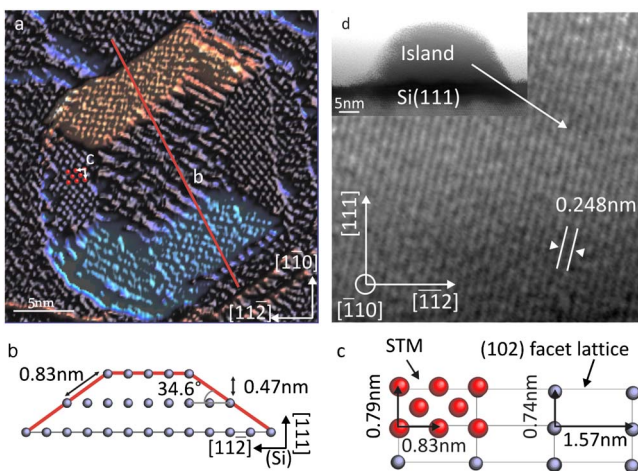


FIG. 2. (Color online) (a) STM image of a Au–Si particle, of 3.5 nm height, in the derivative mode, $I=0.1 \text{ nA}$, $V=+1 \text{ V}$, added balls on the facet correspond to the surface mesh shown in Fig. 2(c). (b) Schematic side view of the silicide island, corresponding to a cut along the line of Fig. 2(a). (c) Lattice of the (102) facet of the silicide as described by von Allmen *et al.* in Ref. 6 and corresponding to STM data. (d) TEM cross sectional views of an Au–Si island, atomic planes are visible, global view of the islands in the inset.

nm was obtained for the out of plane direction [see Fig. 2(b)]. This distance agrees with the metal-rich Au silicides such as $\text{Au}_3\text{Si}\{110\}$, $\text{Au}_7\text{Si}\{111\}$, and the so called Au_xSi -silicide $\{003\}$.⁶ Only the latter silicide has six tilted facets $\{102\}$, forming an angle of 35° with the $\{003\}$ facet. The observed and the expected sizes of the unit cell of the $\{102\}$ facets of this silicide agree perfectly with the STM observations. Identical surface structures were resolved on hemispherical islands. These observations indicate that the surface layer of the islands is composed of the metal rich Au_xSi silicide. The bulk crystallographic structure of the islands was studied with TEM, as illustrated in Fig. 2(d). Several structures and lattice distances have been identified and correspond again to metal-rich Au silicides (Au_3Si , Au_5Si , Au_7Si , and Au_xSi silicides). It is important to mention that the entire island exhibits a silicide structure, as shown in the inset of Fig. 2(d). The existence of a Si skin on the island, previously reported by Calliari *et al.*,⁷ can be excluded in our experimental condition.

The Au–Si phase diagram only shows metastable Au silicides. In a recent study of the high coverage regime of Au on Si(111), one silicide, Au_7Si , was found to be stable at the interface between pure Au and pure Si. This phase, not stable in bulk, can be stabilized at the interface of small islands due to the much smaller interfacial free energy of Au_7Si in comparison to Si and Au.⁸ In contrast to that, the nanometer-sized islands consisting entirely of a Au silicide could be stabilized in our study.

Potential applications in electronics and spintronics are based on the preparation of dense magnetic nanodots. Growth experiments of Co onto the as-prepared templates have been performed in order to transfer the Au–Si islands pattern into a Co film by a selective silicidation process.⁹ Deposition of Co on the locally passivated Si(111) substrates leads to adsorption on both the Si-rich terraces separating the islands and the top of the Au-rich 3D islands. Already at room temperature, Co reacts with Si in the Si-rich regions to form nonmagnetic Co silicides, while the Co on top of the Au-rich islands is less prone to react with Si.¹⁰ The Si outwards diffusion is hindered for temperatures significantly lower than the Au–Si eutectic temperature of 363 °C. The magnetic signal measured *ex situ* at room temperature by magneto-optical Kerr effect (MOKE) on a sample prepared following this selective silicidation scheme is a solid proof that the chemical functionalization was successful, given the same measurement performed on a reference sample with a complete silicidation of the Co film (Fig. 3). Only the islands-functionalized substrate exhibits a magnetic signal, after subtraction of the diamagnetic contributions of silicide film and Si substrate (identical for both samples).

Finally, it is possible to periodically arrange the islands. Self-organized templates were obtained from vicinal Si(111) surfaces by heat treatment under UHV. The vicinal surface transforms into a 1D pattern consisting of equally spaced terraces separated by step bunches as depicted in Fig. 4(a). When using the appropriate parameters for the substrate temperature and the coverage, the nanometer sized metal-rich Au-silicide islands can be grown self-aligned along the step-bunches.⁵ The aligned islands are separated on either side by the 2D Si-rich silicide film. An example of the patterned Si(111) surface with aligned Au–Si islands is given in Fig. 4(b). The island density can be varied between 10^9 and

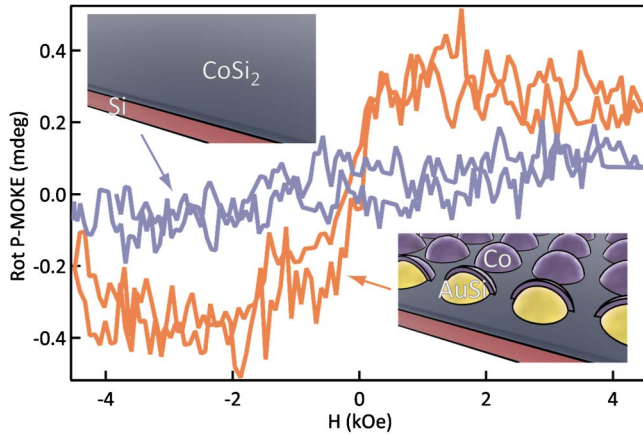


FIG. 3. (Color online) Out-of-plane magnetic hysteresis loops of the MOKE rotation measured in polar configuration at room temperature after the silydation of a 3.6 ML thick Co film deposited on the Au–Si islands-functionalized substrate and on a reference substrate without the islands. Only the islands-functionalized substrate exhibits a magnetic signal, after subtraction of the diamagnetic contributions of silicide film and Si substrate (identical for both samples).

$10^{12}/\text{in.}^2$ through an adequate tuning of the growth parameters, temperature (340–500 °C), and coverage.

In summary, we have shown that stable metal-rich Au silicide islands can be grown and aligned in regular arrays, while between the islands, a Si-rich 2D Au silicide is formed. A chemically inhomogeneous substrate could thus be fabricated, comprised of largely inert Au-rich islands surrounded by reactive Si-rich terraces. This chemical functionalization was used to perform subsequent patterning in electric and

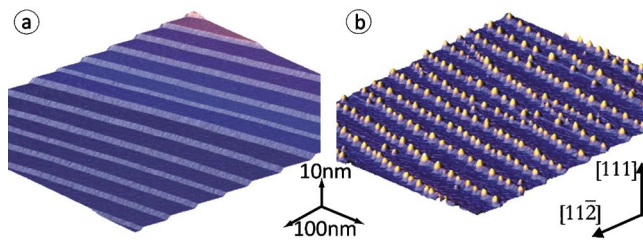


FIG. 4. (Color online) (a) STM image of a vicinal Si(111) surface miscut by 1.5° along $[11\bar{2}]$ direction obtained at room temperature after UHV heat treatment, parallel step bunches are separated by equally sized terraces. (b) STM image ($I=0.5$ nA, $V=+2$ V), taken after deposition of 3.5 ML Au at 370 °C. Au-rich islands are aligned along the step-bunches with a density of 2.5×10^{11} in.^{-2} . Images sizes are 500 nm².

magnetic properties. Oxygen exposure leads to the formation of a high resistive oxide film above the Si-rich 2D wetting layer, while the Au-rich 3D islands stay conductive. Deposition of Co enables to obtain magnetic dots embedded into a nonmagnetic Co silicide film. An increase in the particle density can be obtained by lowering the deposition temperature and/or the vicinity of the Si substrate. Possibly, 2D patterning of Si(111) can be performed on the nanometer scale leading to an increase in the Au island density and to ordered structures via the controlled nucleation of the islands.^{11,12} The as-functionalized substrates also have potential applications in biology by selectively biofunctionalizing the 3D Au-rich islands.

The authors wish to acknowledge financial support of this project through the French Foreign Ministry (PAI-PROCOPE Grant No. 07639QK), the French Research Ministry (ACNN Grant Nos. NR056 and NR017), and the German Academic Exchange Service (Grant No. DAAD D/0333665). The authors are grateful for the skillful technical assistance of Serge Nitsche, CRMCN, for the TEM observations.

- ¹A. Moser, K. Takano, D. T. Margulies, M. Albrecht, Y. Sonobe, Y. Ikeda, S. H. Sun, and E. E. Fullerton, *J. Phys. D: Appl. Phys.* **35**, R157 (2002).
- ²C. Petit, A. Taleb, and M. P. Pileni, *J. Phys. Chem. B* **103**, 1805 (1999).
- ³N. Weiss, T. Cren, M. Epple, S. Rusponi, G. Baudot, S. Rohart, A. Tejada, V. Repain, S. Rousset, P. Ohresser, F. Scheurer, P. Bencok, and H. Brune, *Phys. Rev. Lett.* **95**, 157204 (2005).
- ⁴J. A. Venables, G. Spiller, and M. Hanbücken, *Rep. Prog. Phys.* **47**, 399 (1984).
- ⁵A. Rota, A. Martinez-Gil, G. Agnus, E. Moyen, T. Maroutian, B. Bartenlian, R. Mégy, M. Hanbücken, and P. Beauvillain, *Surf. Sci.* **600**, 1207 (2006).
- ⁶M. Von Allmen, S. S. Lau, M. Mäenpää, and B. Y. Tsaur, *Appl. Phys. Lett.* **36**, 205 (1980).
- ⁷L. Calliari, M. Sancrotti, and L. Braicovich *Phys. Rev. B* **30**, 4885 (1984); J. J. Yeh, J. Hwang, K. Bertness, D. J. Friedman, R. Cao, and I. Lindau, *Phys. Rev. Lett.* **70**, 3768 (1993).
- ⁸J. S. Wu, Y. F. Chen, S. Dhara, C. T. Wu, K. H. Chen, and L. C. Chen, *Appl. Phys. Lett.* **82**, 4468 (2003).
- ⁹A. Fleurence, G. Agnus, T. Maroutian, B. Bartenlian, P. Beauvillain, E. Moyen, and M. Hanbücken, *Appl. Surf. Sci.* **254**, 3147 (2008).
- ¹⁰E. Moyen, M. Macé, C. Léandri, L. Masson, G. Agnus, A. Fleurence, T. Maroutian, W. Wulfhekel, B. Bartenlian, P. Beauvillain, and M. Hanbücken, *J. Phys.: Conf. Ser.* **100**, 072002 (2008).
- ¹¹Y. Homma, P. Finnie, and T. Ogino, *J. Electron Microsc.* **49**, 225 (2000).
- ¹²A. Kraus, R. Kulla, H. Neddermeyer, W. Wulfhekel, D. Sander, T. Maroutian, F. Dulot, A. Martinez-Gil, and M. Hanbücken, *Appl. Surf. Sci.* **234**, 307 (2004).